

Surface Prevalence of Perchlorate Anions at the Air/Aqueous Interface

Wei Hua, Dominique Verreault, and Heather C. Allen*

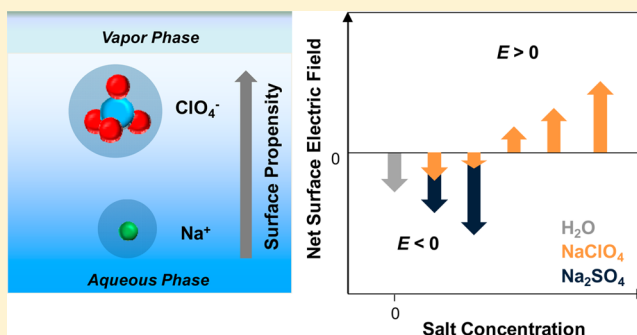
Department of Chemistry & Biochemistry, The Ohio State University, 100 West 18th Avenue, Columbus, Ohio 43210, United States

S Supporting Information

ABSTRACT: Air/aqueous interfaces provide a unique environment for many chemical, environmental, and biological processes. To gain insight, molecular-level understanding of the interfacial water organization and ion distributions at these interfaces is required. Here, the air/aqueous interface of NaClO₄ salt solutions was investigated by means of conventional and heterodyne-detected vibrational sum frequency generation (HD-VSFG) spectroscopy. It is found that perchlorate (ClO₄⁻) ions exist in the interfacial region and prefer to reside on average above their counterions. This finding is inferred from the average orientation of the OH transition dipole moment of interfacial water molecules governed by the direction of the net electric field arising from the interfacial ion distributions.

At the air/aqueous interface of NaClO₄ salt solutions, the net dipole moments of hydrogen-bonded water molecules are oriented preferentially toward the vapor phase. Contrary to some other salts (e.g., sulfates), the presence of ClO₄⁻ may cause a full reversal in the direction of the interfacial electric field at a higher concentration (≥ 1.7 M). Another interpretation for the positive $\text{Im } \chi^{(2)}$ spectra of NaClO₄ salt solutions could be an increase in the population of water species contributing positively to the net OH transition dipole moment. Regardless of the mechanism, this effect becomes even more pronounced with increasing salt concentration.

SECTION: Surfaces, Interfaces, Porous Materials, and Catalysis



The surface propensity and distribution of inorganic ions at the air/aqueous interface and their impact on interfacial water organization have been topics of long-standing interest due to their importance in a wide range of natural and technological processes. For example, various ions play critical roles in the kinetics and mechanisms of heterogeneous chemical reactions at the air/aqueous interface of atmospheric aerosols.^{1–3} The currently adopted molecular view of ion adsorption proposed by molecular dynamics (MD) simulation results suggests that small, nonpolarizable ions like F⁻ and/or multiply charged ions (e.g., SO₄²⁻) are excluded from the air/aqueous interface, while large polarizable halide ions (e.g., Br⁻ and I⁻) have a strong surface propensity.^{4–8} This prediction has since been supported by numerous experimental studies using various surface-sensitive techniques such as ambient pressure X-ray photoelectron spectroscopy (AP-XPS), second harmonic generation (SHG), and vibrational sum frequency generation (VSFG) spectroscopy.^{9–14} Even though the factors and/or driving forces behind ion adsorption are debated, further computational and experimental work on other anions (e.g., SO₄²⁻, NO₃⁻, I⁻) has suggested that the surface propensity of anions correlates inversely with the order of the anion Hofmeister series, CO₃²⁻ > SO₄²⁻ > F⁻ > Cl⁻ > Br⁻ ≈ NO₃⁻ > I⁻ > ClO₄⁻ > SCN⁻.^{6,15–17}

Considering that chaotropic ions such as Br⁻, I⁻, and SCN⁻ are known to be enriched at the air/aqueous interface, the

surface propensity of perchlorate (ClO₄⁻) ions seems somewhat predictable. In fact, the surface enhancement of ClO₄⁻ ions has been postulated as early as 1957 based on the negative surface potential values measured from aqueous NaClO₄ solutions.¹⁸ Despite the fact that ClO₄⁻ ion-induced changes in the conformation of surfactant monolayers and their influence on the vicinal water organization were well-established,¹⁹ molecular-level information about ClO₄⁻ ion surface propensity and its impact on the water hydrogen-bonding network at the bare air/salt solution interface was still lacking. It is only recently that the surface enhancement of ClO₄⁻ ions has been predicted by MD simulations²⁰ and a surface–bulk partitioning model,²¹ as well as demonstrated experimentally using electrospray/mass spectrometry²² and AP-XPS.²⁰ Moreover, it was shown that the presence of ClO₄⁻ ions affects the evaporation mechanism and kinetics at the air/aqueous interface of concentrated NaClO₄ solutions.²³

Aside from its fundamental interest in physical chemistry, ClO₄⁻ has also drawn much attention as an emerging environmental pollutant of drinking water and food.^{24–27} Because of its low surface charge density, it has a reduced affinity for metal cations, a characteristic that makes it highly

Received: September 17, 2013

Accepted: November 25, 2013

Published: November 25, 2013

soluble. As such, ClO_4^- ions tend not to sorb appreciably to minerals and remain exceedingly mobile, thus leading to widespread contamination of natural aqueous systems.²⁸ The environmental occurrence of ClO_4^- ions can be related to either anthropogenic or natural sources such as nitrate mineral deposits and aerosols. It has been suggested that natural perchlorate species could be formed by heterogeneous reactions on chloride-containing aerosols by electric discharge or by exposition to high ozone concentrations.^{29,30} In order to understand these phenomena, it would therefore be helpful to have molecular insight into the interfacial behavior of ClO_4^- ions at the air/aqueous interface.

Despite the fact that the surface propensity of ClO_4^- ions has been explored, their interfacial distribution and that of their counter cations, as well as their influence on the interfacial water hydrogen-bonding network, in particular, the net dipole orientation of water molecules, still remain largely unknown. In this Letter, we employed both conventional and heterodyne-detected vibrational sum frequency generation (HD-VSFG) spectroscopy to gain some further insight into these questions. In contrast to conventional VSFG spectroscopy that measures the squared absolute value of the second-order nonlinear susceptibility ($\chi^{(2)}$), HD-VSFG spectroscopy, by being based on the interference of the sample SFG response with that of a phase reference, can provide both the real (Re) and imaginary (Im) parts of $\chi^{(2)}$. The sign of $\text{Im } \chi^{(2)}$ relates directly not to the orientation of interfacial water molecules but rather to that of the average OH transition dipole moment;^{10,31–34} even though these two parameters are related, the exact molecular details of their connection are currently not well-established. The experimental setup for conventional VSFG and HD-VSFG spectroscopy has been described elsewhere.^{35–38}

Figure 1a shows conventional VSFG spectra of the interfacial region of neat water and NaClO_4 aqueous salt solution measured in the OH stretching region ($3000\text{--}3800\text{ cm}^{-1}$) under the ssp (for sum frequency (s), visible (s), and IR (p) beams, respectively) polarization combination. The interfacial region refers hereafter to the region that lacks inversion symmetry, hence SFG-active. In the case of neat water, only the topmost layers ($\sim 1\text{--}3$) are believed to be responsible for the observed SFG signal, while the adjacent sublayers make little contribution;^{10,39} however, the presence of ions generates an interfacial electric field by forming an ionic double layer that extends the region of noncentrosymmetry. Water organization is directly influenced by the direction and relative strength of the ion-induced electric field in the interfacial region. The perturbation of the interfacial water organization involves both reorientation and restructuring of the water hydrogen-bond network, which, in turn, leads to an increase in the interfacial depth, that is, to a greater number of water molecules probed due to their SFG activity. The neat water VSFG ($|\chi_{\text{eff}}^{(2)}|^2$) spectrum reveals a broad region spanning from 3000 to 3600 cm^{-1} representing water molecules with a broad continuum of hydrogen bond lengths and a narrow band at 3700 cm^{-1} assigned to the distinct dangling OH bond of water molecules located in the topmost layer. In the lower-frequency part of the broad region, it is accepted that hydrogen bonds are relatively strong, and as one moves to higher frequency, the hydrogen-bonding strength weakens significantly. Additional assignments to this broad continuum remain controversial.^{40–44}

The conventional VSFG spectrum of a 1.0 M NaClO_4 aqueous salt solution shows an uneven decrease in SFG signal intensity relative to that of neat water across the entire broad

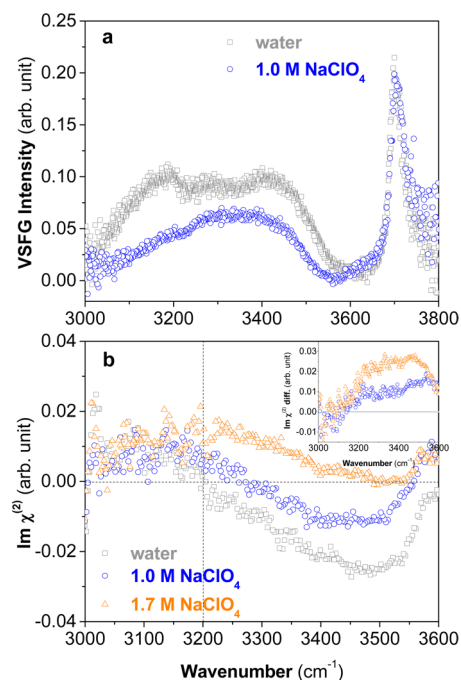


Figure 1. (a) Conventional VSFG $|\chi_{\text{eff}}^{(2)}|^2$ spectra of the air/aqueous interfaces of neat water and 1.0 M NaClO_4 salt solution across the entire OH-stretching region ($3000\text{--}3800\text{ cm}^{-1}$). (b) HD-VSFG $\text{Im } \chi^{(2)}$ spectra of air/aqueous interfaces of 1.0 and 1.7 M NaClO_4 salt solutions. The neat water spectrum is shown as a reference. (Inset) $\text{Im } \chi^{(2)}$ difference spectra ($\text{Im } \chi^{(2)}$ salt spectrum minus $\text{Im } \chi^{(2)}$ neat water spectrum) of the same salt solutions found in (b).

OH stretching region from 3000 to 3600 cm^{-1} , particularly below $\sim 3300\text{ cm}^{-1}$ (Figure 1a). However, no appreciable difference is observed for the dangling OH peak. To the authors' knowledge, no conventional VSFG spectrum of NaClO_4 or any other perchlorate salt solution has been previously reported. The intensity decrease of the broad OH stretching region suggests that the overall population of hydrogen-bonded water species that contribute to the SFG signal may be diminished. Additionally, it provides some evidence that the presence of the ClO_4^- anions in the interfacial region causes a definite perturbation of the water hydrogen-bonding network. In fact, these changes observed in the conventional VSFG spectrum of the NaClO_4 salt solution surface seem to correlate well with those from the corresponding bulk IR and Raman spectra (see the Supporting Information). Previous ATR-IR and Raman studies have shown that the addition of ClO_4^- anions to water leads to (1) a decrease in the absorbance and Raman intensity of lower-frequency bands (~ 3230 and $\sim 3370\text{ cm}^{-1}$) and, concomitantly, (2) the emergence of a new band at higher frequency ($\sim 3600\text{ cm}^{-1}$).^{45–50} The former bands have been assigned to water molecules fully hydrogen-bonded to their nearest neighbors, whereas the latter has been associated with water molecules weakly hydrogen-bonded to the ClO_4^- anions.^{45–50} The changes in these spectral features with salt concentration are believed to be due to the fact that the tetrahedral ClO_4^- anion acts as one of the most effective chaotropic ions by forming weak hydrogen bonds with adjacent water molecules, thereby perturbing the water hydrogen-bonding network. As in the bulk, it is conceivable that ClO_4^- anions affect the network between hydrogen-bonded interfacial water molecules (whether weakly or strongly coordinated) in a similar manner. Moreover,

as with the IR and Raman spectra, a weak band (shoulder) appears upon closer inspection of our VSFG spectrum at $\sim 3620\text{ cm}^{-1}$, suggesting that some of the water molecules weakly bonded to ClO_4^- anions are SFG-active.

Despite a correlation between the spectral changes observed in the broad OH stretching region of the conventional VSFG spectrum and that from the IR and Raman spectra, the contribution of possible interference effects (e.g., interference with the nonresonant background, convolution effects between the real and imaginary parts of the nonlinear susceptibility, etc.) to these changes cannot be completely excluded.⁵¹ For example, the signal enhancement observed at $\sim 3300\text{ cm}^{-1}$ in the conventional VSFG spectrum of CaCl_2 salt solutions³⁷ has been shown to come from convolution effects between the $\text{Re } \chi^{(2)}$ and $\text{Im } \chi^{(2)}$ parts. Hence, to rule out the presence of such effects in the case of NaClO_4 salt solutions, it is advantageous to utilize HD-VSFG spectroscopy.

As mentioned above, the HD-VSFG ($\text{Im } \chi^{(2)}$) spectrum directly provides the sign and thus the net transition dipole moment orientation of SFG-active OH vibrational stretching modes, and the magnitude of the positive or negative intensities reveal the extent of the $\text{O} \rightarrow \text{H}$ dipole orientation, that is, directed either toward or away from the surface, respectively. Note that the interpretation of $\text{Im } \chi^{(2)}$ spectra given herein is based on the *relative* spectral difference between neat water and the aqueous salt solutions. The $\text{Im } \chi^{(2)}$ spectrum of neat water in the OH stretching region shown in Figure 1b is similar to those reported previously by others.^{10,31} The positive sign of the $\text{Im } \chi^{(2)}$ spectrum of neat water in the $3000\text{--}3200\text{ cm}^{-1}$ region suggests that the OH stretching net transition dipole moment is oriented toward the surface; however, the assignments for this region continue to be discussed.^{10,41,42,44} In contrast, the interpretation of the negative band in the $\text{Im } \chi^{(2)}$ spectrum from 3200 to 3600 cm^{-1} is not contested. Although the orientational distribution is likely to be broad, the OH stretches in this frequency range have a net transition dipole moment directed on average toward the isotropic bulk solution.

The $\text{Im } \chi^{(2)}$ spectra of the air/aqueous interface of NaClO_4 salt solutions at different concentrations are shown in Figure 1b. To date, there has been no published accounts of an $\text{Im } \chi^{(2)}$ spectrum from the bare air/aqueous interface of perchlorate salt solutions. Relative to neat water, significant spectral changes, in the form of an enhanced positive signal intensity in the lower-frequency region and a reduced negative intensity for the higher-frequency region, can be seen for both NaClO_4 solutions. Furthermore, at the higher salt concentration, the intensity of the $\text{Im } \chi^{(2)}$ spectrum undergoes a sign reversal in the spectral region from 3200 to 3600 cm^{-1} . The presence of hydronium (H_3O^+) in the NaClO_4 solutions should only play a minor role in the overall change observed in their $\text{Im } \chi^{(2)}$ spectra because of the negligible pH variation relative to neat water (neat water: 5.6; 1.7 M NaClO_4 : 5.9). The change of the $\text{Im } \chi^{(2)}$ spectra of the NaClO_4 solution can be more clearly seen by taking the $\text{Im } \chi^{(2)}$ difference spectra with respect to neat water (inset of Figure 1b). The positive increase in the spectra of NaClO_4 salt solutions observed here can be physically rationalized by having a positive electric field generated between ClO_4^- anions residing on average predominantly above Na^+ cations, closer to the surface. In other words, ClO_4^- ions exhibit a stronger surface preference than Na^+ ions. This molecular picture is consistent with recent MD simulations using a polarizable force field that predicted the formation of an

ionic double layer with a maximal ClO_4^- ion density near the air/aqueous interface.²⁰ A decrease in $\text{ClO}_4^-/\text{Na}^+$ and ClO_4^-/O ratios with increasing depth as obtained by AP-XPS on 1 M NaClO_4 solution further supported the surface enhancement of ClO_4^- ions; however, the presence of a double-layer structure could not be decisively confirmed.²⁰

To explain these results of Figure 1b, various physical scenarios can be invoked. One possible explanation would be that because different water species contribute either negatively or positively to this region of the $\text{Im } \chi^{(2)}$ spectrum, it is quite likely that NaClO_4 addition to water reduces the population of water species contributing negatively, or vice versa, thus allowing the spectrum to become more positive. For instance, the observed net change in the water OH transition dipole moment with increasing salt concentration may result from the increasing population of water molecules weakly bonded to interfacial ClO_4^- anions. These water molecules could have their O–H groups directed on average toward the vapor phase for more surface-active ClO_4^- ions. The OH group contribution then could determine the sign of the $\text{Im } \chi^{(2)}$ spectrum. Yet, because of the symmetry of the ClO_4^- ion, the SFG selection rules would dictate that such water molecules would only make a minor contribution to the overall SFG signal. This seems to be supported by the weak band detected at $\sim 3620\text{ cm}^{-1}$ in the conventional VSFG spectrum. Obviously, as shown by the conventional VSFG spectrum, it is likely that many other water species could be affected by the presence of ClO_4^- anions.²⁰ Unfortunately, current spectroscopic methods do not provide such information.

Another physical scenario that could be put forward to explain the $\text{Im } \chi^{(2)}$ sign reversal involves the generation of a net positive electric field induced by the distribution of ClO_4^- ions and their Na^+ counterions in the interfacial region, that is, by the formation of an ionic double layer within the interface. The ion-induced interfacial electric field, in turn, would cause the reorganization of the interfacial water molecules, which now have their net transition dipole moment more oriented toward the surface. As shown in Figure 1b, the direction and magnitude of the ion-induced electric field at the air/aqueous interface of NaClO_4 salt solutions display a marked concentration dependency. This effect has an impact on the net dipole orientation of interfacial water molecules, mainly those that are weakly hydrogen-bonded ($3200\text{--}3550\text{ cm}^{-1}$ spectral region). The net influence of concentration on the direction and magnitude of the induced electric field is illustrated schematically in Figure 2. At the neat water surface, the electric field is slightly negative due to the net, but weak, orientation of water dipoles pointing toward the aqueous isotropic bulk (seen in the $\text{Im } \chi^{(2)}$ spectrum from 3200 to 3600 cm^{-1}).^{10,31} At low salt concentrations, the distribution of ClO_4^- ions and their Na^+ counterions may generate an additional electric field that counteracts and slightly reduces the magnitude of the overall electric field exerted on water molecules. The net orientation of this field remains however unchanged as the $\text{Im } \chi^{(2)}$ spectra of NaClO_4 salts in the $3200\text{--}3550\text{ cm}^{-1}$ region are still showing a negative intensity. In a slightly more concentrated regime, the magnitude of the ClO_4^- -induced electric field eventually gives rise to a strong enough electrical field capable of completely inverting the net dipole orientation of interfacial water molecules, thus resulting in purely positive $\text{Im } \chi^{(2)}$ spectra. The presence of a net positive electric field at the surface of NaClO_4 and other perchlorate salt solutions is supported by

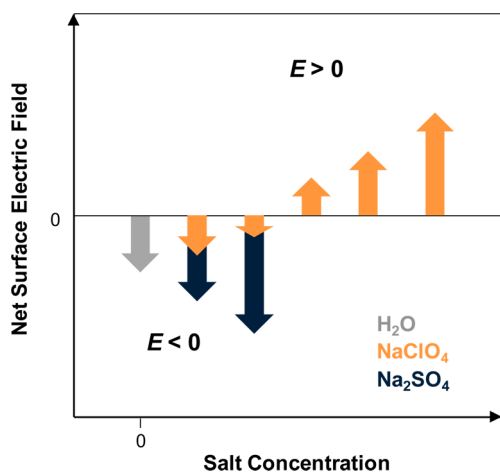


Figure 2. Diagram qualitatively demonstrating the salt concentration dependence of the magnitude and direction of the overall electric field as exemplified by NaClO_4 and Na_2SO_4 salt solutions.

experimentally measured negative surface potentials (recalling that $E = -\nabla V$).^{18,52,53}

Such a complete reversal of the average orientation of the net transition dipole moment of weakly hydrogen-bonded interfacial water molecules observed here for ClO_4^- has so far not been reported for other chaotropic ions including the surface-enhanced I^- ions.^{10,36,37,54} It is noteworthy that although SCN^- , ClO_4^- , and I^- ions are all monovalent anions, the overall line shape of their conventional VSG spectra and their variation with concentration increase differ significantly.^{11,55} In comparison to ClO_4^- , which displays a decreasing intensity across the entire OH stretching region, SCN^- and I^- ions show concurrent decrease and increase at ~ 3200 and ~ 3450 cm^{-1} , respectively, indicative of a very different disordering effect on the interfacial water network. A shape anisotropy effect between these anions (i.e., tetrahedral (ClO_4^-) versus spherical (I^-) versus linear (SCN^-)) may be largely responsible for this difference. Interestingly, an enhanced negative interfacial electric field inferred from the $\text{Im } \chi^{(2)}$ spectrum of the large polarizable sulfate (SO_4^{2-}) has also been previously reported.^{37,54} However, the direction of the induced electric field for SO_4^{2-} and ClO_4^- (Figure 2) and the surface propensity of these two tetrahedral-structured oxyanions in the interfacial region are very different. This suggests that, in addition to the shape/geometry effect, the charge effect of the ions plays a key role in determining the ion distribution and water organization at air/aqueous salt solution interfaces.

In summary, from the HD-VSG results obtained here, it is clear that ClO_4^- ions are present at the air/aqueous interface of NaClO_4 salt solutions and that, as a result, the interfacial water structure is significantly reorganized. ClO_4^- ions reside preferentially on average above their Na^+ counterions. This was inferred from the positive direction of the net OH transition dipole moment of interfacial water molecules on average more toward the surface. An increase in salt concentration leads to the complete sign reversal of the $\text{Im } \chi^{(2)}$ spectrum. Possible scenarios explaining this effect include the increase in population of water species contributing positively to the $\text{Im } \chi^{(2)}$ spectrum or the generation of a net positive electric field induced by the creation of an ionic double layer in the interfacial region. Although the true molecular origins of this concentration dependency remain at present somewhat speculative, previous surface potential and XPS

measurements tend to support the latter interpretation. To our knowledge, this is the first investigation of water organization at the air/aqueous interface of a NaClO_4 salt solution using conventional VSG and HD-VSG spectroscopy. Nevertheless, further theoretical and experimental efforts are needed to fully decipher the effects of concentration and cation identity on the distribution of ClO_4^- ions and its accompanying counter cations.

■ ASSOCIATED CONTENT

📄 Supporting Information

Experimental procedures for sample preparation, description of conventional VSG and HD-VSG, as well as Raman and IR spectroscopy. Conventional VSG spectra at the air/aqueous interface of neat water and NaClO_4 salt solution in the CH stretching region ($2800\text{--}3000$ cm^{-1}). GaAs profile and conventional VSG $|\chi_{\text{eff}}^{(2)}|^2$ and HD-VSG $\text{Im } \chi^{(2)}$ spectra of neat water obtained through the entire experimental period demonstrating system and phase stability. The $|\chi^{(2)}|^2$ power spectra and $\text{Re } \chi^{(2)}$ spectra deduced from HD-VSG results of water molecules at air/aqueous interface of NaClO_4 salt solutions. Raman and IR spectra of NaClO_4 salt solutions. This material is available free of charge via the Internet at <http://pubs.acs.org>.

■ AUTHOR INFORMATION

✉ Corresponding Author

*E-mail: allen@chemistry.ohio-state.edu.

📄 Notes

The authors declare no competing financial interest.

■ ACKNOWLEDGMENTS

The authors acknowledge the NSF-CHE (Grant No. 1111762) for funding this work. W.H. acknowledges a Presidential Fellowship from The Ohio State University.

■ REFERENCES

- (1) Knipping, E. M.; Lakin, M. J.; Foster, K. L.; Jungwirth, P.; Tobias, D. J.; Gerber, R. B.; Dabdub, D.; Finlayson-Pitts, B. J. Experiments and Simulations of Ion-Enhanced Interfacial Chemistry on Aqueous NaCl Aerosols. *Science* **2000**, *288*, 301–306.
- (2) Finlayson-Pitts, B. J.; Pitts, J. N., Jr. *Chemistry of the Upper and Lower Atmosphere: Theory, Experiments and Applications*; Academic Press: San Diego, CA, 2000.
- (3) Finlayson-Pitts, B. J. Reactions at Surfaces in the Atmosphere: Integration of Experiments and Theory as Necessary (but Not Necessarily Sufficient) for Predicting the Physical Chemistry of Aerosols. *Phys. Chem. Chem. Phys.* **2009**, *11*, 7760–7779.
- (4) Jungwirth, P.; Tobias, D. J. Molecular Structure of Salt Solutions: A New View of the Interface with Implications for Heterogeneous Atmospheric Chemistry. *J. Phys. Chem. B* **2001**, *105*, 10468–10472.
- (5) Dang, L. X. Computational Study of Ion Binding to the Liquid Interface of Water. *J. Phys. Chem. B* **2002**, *106*, 10388–10394.
- (6) Jungwirth, P.; Tobias, D. J. Specific Ion Effects at the Air/Water Interface. *Chem. Rev.* **2006**, *106*, 1259–1281.
- (7) Tobias, D. J.; Stern, A. C.; Baer, M. D.; Levin, Y.; Mundy, C. J. Simulation and Theory of Ions at Atmospherically Relevant Aqueous Liquid–Air Interfaces. *Annu. Rev. Phys. Chem.* **2013**, *64*, 339–359.
- (8) Jungwirth, P.; Curtis, J. E.; Tobias, D. J. Polarizability and Aqueous Solvation of the Sulfate Dianion. *Chem. Phys. Lett.* **2003**, *367*, 704–710.
- (9) Bian, H.-t.; Feng, R.-r.; Xu, Y.-y.; Guo, Y.; Wang, H.-f. Increased Interfacial Thickness of the NaF, NaCl and NaBr Salt Aqueous Solutions Probed with Non-Resonant Surface Second Harmonic Generation (SHG). *Phys. Chem. Chem. Phys.* **2008**, *10*, 4920–4931.

- (10) Ji, N.; Ostroverkhov, V.; Tian, C. S.; Shen, Y. R. Characterization of Vibrational Resonances of Water–Vapor Interfaces by Phase-Sensitive Sum-Frequency Spectroscopy. *Phys. Rev. Lett.* **2008**, *100*, 096102/1–096102/4.
- (11) Liu, D.; Ma, G.; Levering, L. M.; Allen, H. C. Vibrational Spectroscopy of Aqueous Sodium Halide Solutions and Air–Liquid Interfaces: Observation of Increased Interfacial Depth. *J. Phys. Chem. B* **2004**, *108*, 2252–2260.
- (12) Mucha, M.; Frigato, T.; Levering, L. M.; Allen, H. C.; Tobias, D. J.; Dang, L. X.; Jungwirth, P. Unified Molecular Picture of the Surfaces of Aqueous Acid, Base, and Salt Solutions. *J. Phys. Chem. B* **2005**, *109*, 7617–7623.
- (13) Raymond, E. A.; Richmond, G. L. Probing the Molecular Structure and Bonding of the Surface of Aqueous Salt Solutions. *J. Phys. Chem. B* **2004**, *108*, 5051–5059.
- (14) Cheng, M. H.; Callahan, K. M.; Margarella, A. M.; Tobias, D. J.; Hemminger, J. C.; Bluhm, H.; Krisch, M. J. Ambient Pressure X-ray Photoelectron Spectroscopy and Molecular Dynamics Simulation Studies of Liquid/Vapor Interfaces of Aqueous NaCl, RbCl, and RbBr Solutions. *J. Phys. Chem. C* **2012**, *116*, 4545–4555.
- (15) Zhang, Y. J.; Cremer, P. S. Chemistry of Hofmeister Anions and Osmolytes. *Annu. Rev. Phys. Chem.* **2010**, *61*, 63–83.
- (16) Tobias, D. J.; Hemminger, J. C. Chemistry — Getting Specific about Specific Ion Effects. *Science* **2008**, *319*, 1197–1198.
- (17) Parsons, D. F.; Bostrom, M.; Lo Nostro, P.; Ninham, B. W. Hofmeister Effects: Interplay of Hydration, Nonelectrostatic Potentials, and Ion Size. *Phys. Chem. Chem. Phys.* **2011**, *13*, 12352–12367.
- (18) Randles, J. E. B. Ionic Hydration and the Surface Potential of Aqueous Electrolytes. *Discuss. Faraday Soc.* **1957**, *24*, 194–199.
- (19) Gurau, M. C.; Lim, S.-M.; Castellana, E. T.; Albertorio, F.; Kataoka, S.; Cremer, P. S. On the Mechanism of the Hofmeister Effect. *J. Am. Chem. Soc.* **2004**, *126*, 10522–10523.
- (20) Baer, M. D.; Kuo, I. F. W.; Bluhm, H.; Ghosal, S. Interfacial Behavior of Perchlorate versus Chloride Ions in Aqueous Solutions. *J. Phys. Chem. B* **2009**, *113*, 15843–15850.
- (21) Pegram, L. M.; Record, M. T. Hofmeister Salt Effects on Surface Tension Arise from Partitioning of Anions and Cations between Bulk Water and the Air–Water Interface. *J. Phys. Chem. B* **2007**, *111*, 5411–5417.
- (22) Cheng, J.; Vecitis, C. D.; Hoffmann, M. R.; Colussi, A. J. Experimental Anion Affinities for the Air/Water Interface. *J. Phys. Chem. B* **2006**, *110*, 25598–25602.
- (23) Drisdell, W. S.; Saykally, R. J.; Cohen, R. C. Effect of Surface Active Ions on the Rate of Water Evaporation. *J. Phys. Chem. C* **2010**, *114*, 11880–11885.
- (24) Urbansky, E. T. Perchlorate as an Environmental Contaminant. *Environ. Sci. Pollut. Res.* **2002**, *9*, 187–192.
- (25) *Perchlorate: Environmental Occurrence, Interactions and Treatment*; Gu, G., Coates, J. D., Eds.; Springer: New York, 2006.
- (26) Dasgupta, P. K.; Dyke, J. V.; Kirk, A. B.; Jackson, W. A. Perchlorate in the United States. Analysis of Relative Source Contributions to the Food Chain. *Environ. Sci. Technol.* **2006**, *40*, 6608–6614.
- (27) Rajagopalan, S.; Anderson, T.; Cox, S.; Harvey, G.; Cheng, Q.; Jackson, W. A. Perchlorate in Wet Deposition across North America. *Environ. Sci. Technol.* **2009**, *43*, 616–622.
- (28) Parker, D. R.; Seyfferth, A. L.; Reese, B. K. Perchlorate in Groundwater: A Synoptic Survey of “Pristine” Sites in the Conterminous United States. *Environ. Sci. Technol.* **2008**, *42*, 1465–1471.
- (29) Dasgupta, P. K.; Martinelango, P. K.; Jackson, W. A.; Anderson, T. A.; Tian, K.; Tock, R. W.; Rajagopalan, S. The Origin of Naturally Occurring Perchlorate: The Role of Atmospheric Processes. *Environ. Sci. Technol.* **2005**, *39*, 1569–1575.
- (30) Rao, B.; Anderson, T. A.; Redder, A.; Jackson, W. A. Perchlorate Formation by Ozone Oxidation of Aqueous Chlorine/Oxy-Chlorine Species: Role of Cl_2O_y Radicals. *Environ. Sci. Technol.* **2010**, *44*, 2961–2967.
- (31) Nihonyanagi, S.; Yamaguchi, S.; Tahara, T. Direct Evidence for Orientational Flip–Flop of Water Molecules at Charged Interfaces: A Heterodyne-Detected Vibrational Sum Frequency Generation Study. *J. Chem. Phys.* **2009**, *130*, 204704/1–204704/5.
- (32) Stipokin, I. V.; Weeraman, C.; Pieniazek, P. A.; Shalhout, F. Y.; Skinner, J. L.; Benderskii, A. V. Hydrogen Bonding at the Water Surface Revealed by Isotopic Dilution Spectroscopy. *Nature* **2011**, *474*, 192–195.
- (33) Pool, R. E.; Versluis, J.; Backus, E. H. G.; Bonn, M. Comparative Study of Direct and Phase-Specific Vibrational Sum-Frequency Generation Spectroscopy: Advantages and Limitations. *J. Phys. Chem. B* **2011**, *115*, 15362–15369.
- (34) Feng, R.-r.; Guo, Y.; Lue, R.; Velarde, L.; Wang, H.-f. Consistency in the Sum Frequency Generation Intensity and Phase Vibrational Spectra of the Air/Neat Water Interface. *J. Phys. Chem. A* **2011**, *115*, 6015–6027.
- (35) Chen, X. K.; Hua, W.; Huang, Z. S.; Allen, H. C. Interfacial Water Structure Associated with Phospholipid Membranes Studied by Phase-Sensitive Vibrational Sum Frequency Generation Spectroscopy. *J. Am. Chem. Soc.* **2010**, *132*, 11336–11342.
- (36) Hua, W.; Chen, X. K.; Allen, H. C. Phase-Sensitive Sum Frequency Revealing Accommodation of Bicarbonate Ions, and Charge Separation of Sodium and Carbonate Ions within the Air/Water Interface. *J. Phys. Chem. A* **2011**, *115*, 6233–6238.
- (37) Hua, W.; Jubb, A. M.; Allen, H. C. Electric Field Reversal of Na_2SO_4 , $(\text{NH}_4)_2\text{SO}_4$, and Na_2CO_3 Relative to CaCl_2 and NaCl at the Air/Aqueous Interface Revealed by Heterodyne Detected Phase-Sensitive Sum Frequency. *J. Phys. Chem. Lett.* **2011**, *2*, 2515–2520.
- (38) Hua, W.; Verreault, D.; Adams, E. M.; Huang, Z. S.; Allen, H. C. Impact of Salt Purity on Interfacial Water Organization Revealed by Conventional and Phase-Sensitive Sum Frequency Generation Spectroscopy. *J. Phys. Chem. C* **2013**, *117*, 19577–19585.
- (39) Morita, A.; Hynes, J. T. A Theoretical Analysis of the Sum Frequency Generation Spectrum of the Water Surface. *Chem. Phys.* **2000**, *258*, 371–390.
- (40) Tian, C. S.; Shen, Y. R. Sum-Frequency Vibrational Spectroscopic Studies of Water/Vapor Interfaces. *Chem. Phys. Lett.* **2009**, *470*, 1–6.
- (41) Sovago, M.; Campen, R. K.; Bakker, H. J.; Bonn, M. Hydrogen Bonding Strength of Interfacial Water Determined with Surface Sum-Frequency Generation. *Chem. Phys. Lett.* **2009**, *470*, 7–12.
- (42) Ishiyama, T.; Morita, A. Analysis of Anisotropic Local Field in Sum Frequency Generation Spectroscopy with the Charge Response Kernel Water Model. *J. Chem. Phys.* **2009**, *131*, 244714–244717.
- (43) Raymond, E. A.; Tarbuck, T. L.; Brown, M. G.; Richmond, G. L. Hydrogen-Bonding Interactions at the Vapor/Water Interface Investigated by Vibrational Sum-Frequency Spectroscopy of $\text{HOD}/\text{H}_2\text{O}/\text{D}_2\text{O}$ Mixtures and Molecular Dynamics Simulations. *J. Phys. Chem. B* **2003**, *107*, 546–556.
- (44) Pieniazek, P. A.; Tainter, C. J.; Skinner, J. L. Surface of Liquid Water: Three-Body Interactions and Vibrational Sum-Frequency Spectroscopy. *J. Am. Chem. Soc.* **2011**, *133*, 10360–10363.
- (45) Walrafen, G. E. Raman Spectral Studies of Effects of Perchlorate Ion on Water Structure. *J. Chem. Phys.* **1970**, *52*, 4176–4198.
- (46) Rodgers, G. E.; Plane, R. A. A Raman Spectrophotometric Study of the Effect of *N,N*-Dimethylformamide and the Electrolytes NaClO_4 , $\text{Zn}(\text{ClO}_4)_2$, NaNO_3 , and $\text{Zn}(\text{NO}_3)_2$ on the Structure of Liquid Water. *J. Chem. Phys.* **1975**, *63*, 818–829.
- (47) Stangret, J.; Kostrowicki, J. IR-Study of Aqueous Metal Perchlorate Solutions. *J. Solution Chem.* **1988**, *17*, 165–173.
- (48) Rull, F. Structural Investigation of Water and Aqueous Solutions by Raman Spectroscopy. *Pure Appl. Chem.* **2002**, *74*, 1859–1870.
- (49) Saitow, K.; Kobayashi, K.; Nishikawa, K. How Are Hydrogen Bonds Perturbed in Aqueous NaClO_4 Solutions Depending on the Concentration?: A Near Infrared Study of Water. *J. Solution Chem.* **2004**, *33*, 689–698.
- (50) Chen, Y.; Zhang, Y. H.; Zhao, L. J. ATR-FTIR Spectroscopic Studies on Aqueous LiClO_4 , NaClO_4 , and $\text{Mg}(\text{ClO}_4)_2$ Solutions. *Phys. Chem. Chem. Phys.* **2004**, *6*, 537–542.

(51) Tian, C. S.; Ji, N.; Waychunas, G. A.; Shen, Y. R. Interfacial Structures of Acidic and Basic Aqueous Solutions. *J. Am. Chem. Soc.* **2008**, *130*, 13033–13039.

(52) Frumkin, A. Phasengrenzkräfte und Adsorption an der Trennungsfläche Luft/Lösung Anorganischer Electrolyte. *Z. Phys. Chem.* **1924**, *109*, 34–48.

(53) Verreault, D.; Allen, H. C. Bridging the Gap between Microscopic and Macroscopic Views of Air/Aqueous Salt Interfaces. *Chem. Phys. Lett.* **2013**, *586*, 1–9.

(54) Tian, C. S.; Byrnes, S. J.; Han, H. L.; Shen, Y. R. Surface Propensities of Atmospherically Relevant Ions in Salt Solutions Revealed by Phase-Sensitive Sum Frequency Vibrational Spectroscopy. *J. Phys. Chem. Lett.* **2011**, *2*, 1946–1949.

(55) Viswanath, P.; Motschmann, H. Effect of Interfacial Presence of Oriented Thiocyanate on Water Structure. *J. Phys. Chem. C* **2008**, *112*, 2099–2103.